Talanta 94 (2012) 257–262

Contents lists available at SciVerse ScienceDirect

Talanta

journal homepage: www.elsevier.com/locate/talanta

A near-infrared-emitting CdTe/CdS core/shell quantum dots-based OFF–ON fluorescence sensor for highly selective and sensitive detection of Cd^{2+}

Rijun Gui, Xueqin An*, Hongjuan Su, Weiguo Shen, Zhiyun Chen, Xiaoyong Wang

Department of Physical Chemistry, School of Chemistry and Molecular Engineering, East China University of Science and Technology, Meilong Road 130, Shanghai 200237, PR China

ARTICLE INFO

Article history:
Received 4 December 2011
Received in revised form 15 March 2012
Accepted 22 March 2012
Available online 29 March 2012

Keywords:
Quantum dots
Sensor
Fluorescence quenching
Fluorescence enhancement

ABSTRACT

A near-infrared-emitting CdTe/CdS core/shell quantum dots (QDs)-based photoluminescence (PL) sensor was designed and applied for highly selective and sensitive detection of Cd^{2+}. This sensor was based on a PL "OFF–ON" mode. First, the addition of ammonium pyrrolidine dithiocarbamate (APDC) led to remarked PL quenching of QDs. Second, PL of APDC surface modified QDs (QDs-APDC) was gradually restored with the each increment of Cd^{2+} concentration. Experimental results showed that PL of QDs-APDC was near proportional upon the addition of Cd^{2+} in the range from 0.1 to 2 μM with a good correlation coefficient of 0.9989. The limit of detection of this proposed method was 6 nM. Interferential experiments confirmed that this sensor of Cd^{2+} was highly selective over other metal ions. To further investigate perfect analysis performance, this sensor was favorably utilized to determine Cd^{2+} in tap water, river water and liposome solutions.

1. Introduction

Contamination with heavy metal ions poses a serious threat to the environment and human health. In particular, cadmium ion (Cd^{2+}) is widely utilized in many industrial processes, which results in high cadmium contamination in soil, water and food, and has attracted great concerns [1,2]. In addition, Cd^{2+} could accumulate in kidney, liver, lung, and so forth, and cause a variety of acute or chronic effects on human health [3]. Thus, it is urgent to achieve a probe that can provide facile and rapid on-site evaluation of Cd^{2+} ions. Although traditional analytical techniques, including inductively coupled plasma mass spectroscopy, microparticle-induced X-ray emission, atomic adsorption spectrometry, electron paramagnetic resonance and synchrotron radiation X-ray spectrometry have been developed in recent years, these techniques are time-consuming and expensive for the measurement of Cd^{2+} due to requiring complicated sample preparation and sophisticated instruments.

The spectrofluorimetric method seems to be a promising alternative for the detection of metal ions because of its appealing advantages, such as high sensitivity, simplicity and low cost. During the past decade, synthetic organic dyes-based fluorescence sensors of Cd^{2+} have been designed. Cheng et al. developed a BODIPY fluorophore-based fluorescence sensor for Cd^{2+} in aqueous solution and living cell, in company with a low detection concentration of 10 μM [4]. Bao et al. utilized 8-hydroxy-2-methyl-bisquinoline as a sensor of Cd^{2+}. The detection limit of Cd^{2+} ions was determined at least down to 20 nM by fluorimetric assay [5]. Most recently, Oztekin et al. reported electrochemical sensors for voltammetric determination of Cd^{2+} using 1,10-phenanthroline modified glassy carbon electrode [6]. In these sensor systems, relatively complicated synthesis and purification, low photoluminescence (PL) quantum yields (QYs) and solubility in aqueous media, and poor photostability of organic fluorophores partly restrained their practical applications.

However, colloidal semiconductor nanocrystals (also referred to as quantum dots, QDs) probably overcome this limitation. Unique properties of QDs, such as high-quality PL, the broad excitation and size-tunable PL spectrum, relatively high QYs and photochemical stability, allow QDs-based PL sensors to generate a distinct target signal for qualitative or quantificational analysis of various substances [7–16]. For QDs-based sensing of metal ions, previous reports have extensively adopted a PL quenching mode, where various factors rather than analytes could induce the ultimate PL "OFF" state. The problem would affect sensitive and selective detection of analytes [17–20]. Compared to the PL quenching mode, a PL "turn-on" mode should be preferable because the PL "OFF–ON" conversion in the "turn-on" mode could effectively reduce the change of false positives and is more amenable to multiplexing, such as the simultaneous usage of several detectors that uniquely respond to various analytes [21].

Nevertheless, to the best of our knowledge, very rare studies of QDs-based PL "turn-on" sensors were reported [22–26]. For instance, Santra et al. designed selective detection of Cd^{2+} by

* Corresponding author. Tel.: +86 21 6425 0804; fax: +86 21 6425 2012.
E-mail addresses: jacky_0538@163.com (R. Gui), anxueqin@ecust.edu.cn (X. An).

0039-9140/$ – see front matter © 2012 Elsevier B.V. All rights reserved.
http://dx.doi.org/10.1016/j.talanta.2012.03.036

controlling the electron transfer pathways of N-containing crown ether functionalized QDs [25]. Ruedas-Rama and Hall detected Zn^{2+} utilizing the host–guest interaction between azamacrocycles conjugated-QDs and analytes [26]. In these sensors, a relatively complicated surface modification on QDs was required and PL wavelength of proposed QDs was below 650 nm, which limited their selectivity, stability and applicability to real sample [27]. By contrast, QDs with near-infrared (NIR)-emitting between 650 and 900 nm are of particular interest for PL sensing of ions because autofluorescence and absorbance of many molecules could be lessened to the minima in this region [18,28]. To date, NIR-emitting QDs-based PL sensors for metal ions are still rarely reported [29].

Herein, NIR-emitting CdTe/CdS core/shell QDs prepared in aqueous media with 3-mercaptopropionic acid (MPA) as a stabilizer, were modified by ammonium pyrrolidine dithiocarbamate (APDC) to obtain a PL "OFF–ON" sensor for the detection of Cd^{2+}. The designed sensor works in principles as exhibited in Scheme 1. First, the addition of APDC to water-soluble CdTe/CdS QDs solution gave rise to a marked quenching of the initial PL of QDs. The PL quenching is attributed to the chemical etching of the surface of QDs by APDC, which destroyed Cd–thiol layers and resulted in the formation of Cd–APDC complex. Partial loss of Cd–thiol layers decreased surface passivation of QDs and induced PL quenching. Then, the intentional introduction of Cd^{2+} into this APDC-modified QDs solution partially restored the PL. The PL enhancement derives from the occurrence of Cd–thiol passivation layers on the surface of QDs. In addition, this proposed method presented highly selective and sensitive PL response over other common metal ions, and could be developed as a perfect PL sensor for the detection of Cd^{2+} in single or complex solutions.

2. Materials and methods

2.1. Chemicals

Tellurium power (99.999%, ~200 mesh) and MPA were purchased from Aldrich. $CdCl_2{\cdot}2.5H_2O$ (99%), $NaBH_4$ (99%), thiourea and other chemicals were obtained from Shanghai Reagent Company of China. Other chemicals were of analytical grade and all chemicals were utilized directly as received without any purification. The ultrapure water with a resistivity of 18.2 ΩM cm^{-1} (Millipore Simplicity, USA) was used in all experiments. The 10 mM of phosphate buffer solution (PBS, pH 7.0) was prepared by mixing 6.1 mM of Na_2HPO_4 and 3.9 mM of KH_2PO_4 together.

2.2. Apparatus

UV–vis spectrum was recorded with a UV-2450 spectrophotometer (Shimadzu, Japan). Fluorescence spectra measurements were performed with a FLSP 920 fluorescence spectrophotometer (Edinburgh Instruments, U.K.) with a xenon lamp used for excitation at room temperature. The fluorescence lifetime study was performed using an Edinburgh FL nF900 mode single-photon counting system equipped with a Hydrogen lamp as the excitation resource. Powder X-ray diffraction (Siemens, Germany) was obtained with wide-angle X-ray scattering, using a D5005 X-ray powder diffractometer equipped with graphite monochromatized Cu Kα radiation (λ = 1.54056 Å). XRD sample was prepared by depositing QDs powder on a piece of Si (1 0 0) wafer. The composition for sample solutions was measured by means of inductively coupled plasma atomic emission spectroscopy (ICP-AES, Integra XL, Australia) using a standard HCl/HNO_3 digestion.

2.3. Synthesis of MPA-capped CdTe QDs

NaHTe precursor was synthesized using a modified version of the method of Gu et al. [30]. Typically, 0.5 mmol of Te and 2 mmol of $NaBH_4$ were loaded in a three-necked flask, where the air was pumped off and replaced with N_2. Then 10 mL of ultrapure water was added with a syringe and reaction mixture was heated at 80 °C for 30 min to obtain a deep-red clear solution. The as-prepared NaHTe solution was immediately used or stored for further use under the ambience of N_2.

MPA-capped CdTe QDs were prepared by a modified procedure of Zou et al. [31]. Briefly, 0.25 mmol of Cd^{2+} and 0.45 mmol of MPA were placed into a three-necked flask to form 50 mL of homogeneous aqueous solution, adjusting the pH of the solution to 12.0 by dropwise addition of 1.0 M NaOH. Under the protection of N_2, freshly prepared 0.025 mmol of NaHTe was swiftly injected into this solution at room temperature. Then, this solution was heated to reflux with a condenser attached at 100 °C. Aliquots of reaction solution were taken out at different time intervals to record temporal evolution of UV–vis and PL spectra. When reaction time reached 6 h, expected PL wavelength was observed and following operation was to remove the heating source and cool this solution to room temperature. Afterward, the as-prepared CdTe QDs was concentrated by circumrotate evaporation, precipitated with 2-propanol and collected by centrifugation. Colloidal precipitates were dried in vacuum at 60 °C, and re-dispersed in aqueous solution for further applications in subsequent experiments.

2.4. Synthesis of MPA-capped CdTe/CdS core/shell QDs

In this study, a modified version of the method of Fang et al. was adopted to synthesize MPA-capped CdTe/CdS core/shell QDs [32]. In detail, 20 mL of aqueous solution, containing 0.01 mmol of Cd^{2+}, 0.02 mmol of MPA and 0.01 mmol of thiourea, was loaded in a three-necked flask, the pH of the mixture was adjusted to 7.0. And then, the final pH was adjusted to 11.5 after adding 0.04 mmol of MPA and 0.02 mmol of CdTe QDs aqueous solution. The concentration of QDs was calculated by empirical mathematical functions reported by Yu et al. [33]. The air in this system was pumped off and replaced with N_2. Afterward, reaction mixture was heated to reflux at 100 °C under N_2 atmosphere. Aliquots of reaction production were taken at different growth time of CdS shells to record UV–vis and fluorescence spectra. After growing for 4 h, the as-prepared QDs were collected by the method referred above, and dispersed in PBS.

2.5. Sample preparation of PL quenching and enhancement

The as-prepared MPA-capped CdTe/CdS QDs was dispersed in 10 mM of PBS (pH 7.0), and the concentration of QDs (C_{QDs}) was adjusted to 20 nM. Then, APDC aqueous solution was added into this PBS of QDs to obtain a series of homogeneous mixtures with the each increment of APDC concentration (C_{APDC}) from 0 to 5 μM. These mixtures were applied to investigate PL quenching behavior of QDs. In addition, PBS of QDs with the addition of 4 μM of APDC was utilized to evaluate PL enhancement performance of QDs-APDC by intentional introduction of Cd^{2+} in the concentration range ($C_{Cd^{2+}}$) from 0 to 2 μM. Therein, all PL spectra measurements at room temperature were performed by incubating sample solutions for 10 min in a black place to obtain final PL intensities.

3. Results and discussion

3.1. Characterization of CdTe/CdS QDs

According to previous reports, the epitaxial deposition of a compressive CdS layer onto a soft nanocrystalline CdTe core to form

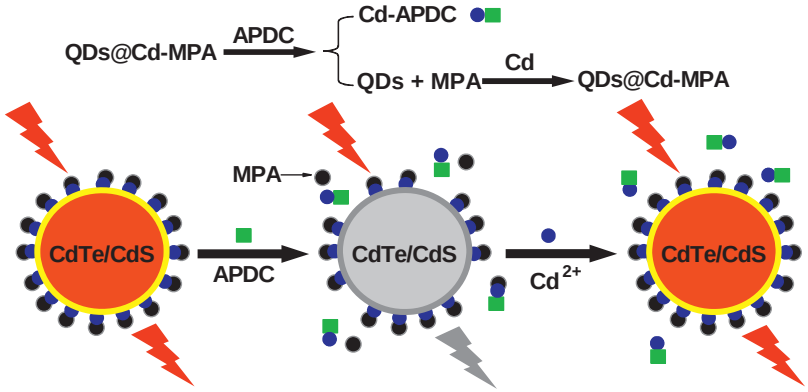

Scheme 1. Schematic representation of the preparation of CdTe/CdS core/shell QDs-based "OFF–ON" fluorescence sensor of Cd^{2+} ions.

a lattice-mismatched type-II core/shell heterostructure QDs could dramatically result in giant spectral red shifts and acquire high-quality luminescent properties simultaneously [34]. Thus, to get NIR-emitting QDs, it is more reasonable to synthesize CdTe/CdS core/shell structures than to directly prepare sole core CdTe at the same condition. UV–vis absorption and PL emission spectra of sole core CdTe and CdTe/CdS core/shell QDs were shown in Fig. 1a and b. By extending reflux time to maintain the growth of CdS layers around CdTe QDs, both absorption and PL wavelength of CdTe/CdS QDs red shifted remarkably. After the growth time reached 4 h (sample D), the maximal PL wavelength was 738 nm. The full width at half maximum (FWHM) is about 75 nm and symmetric, which suggested that these as-prepared NIR-emitting CdTe/CdS QDs were near monodisperse and homogeneous, and could be utilized as a perfect chromophore in subsequent experiments.

In addition, powder XRD patterns for CdTe cores and CdTe/CdS heterostructures were exhibited in Fig. 1c. The XRD pattern of CdTe QDs consists of characteristic peaks of cubic zinc-blende CdTe. When CdS shells are grown around CdTe, general pattern of the cubic lattice is maintained in core/shell structures, but diffraction peaks shift to larger angles and become slightly narrow, consistent with the smaller lattice constant for CdS compared with CdTe. This narrowing behavior of diffraction peaks is attributed to the overcoating of shell materials, which indicates that the crystalline domain is larger for core/shell structures and provides a direct evidence for epitaxial growth [35]. In general, a homogeneous alloy

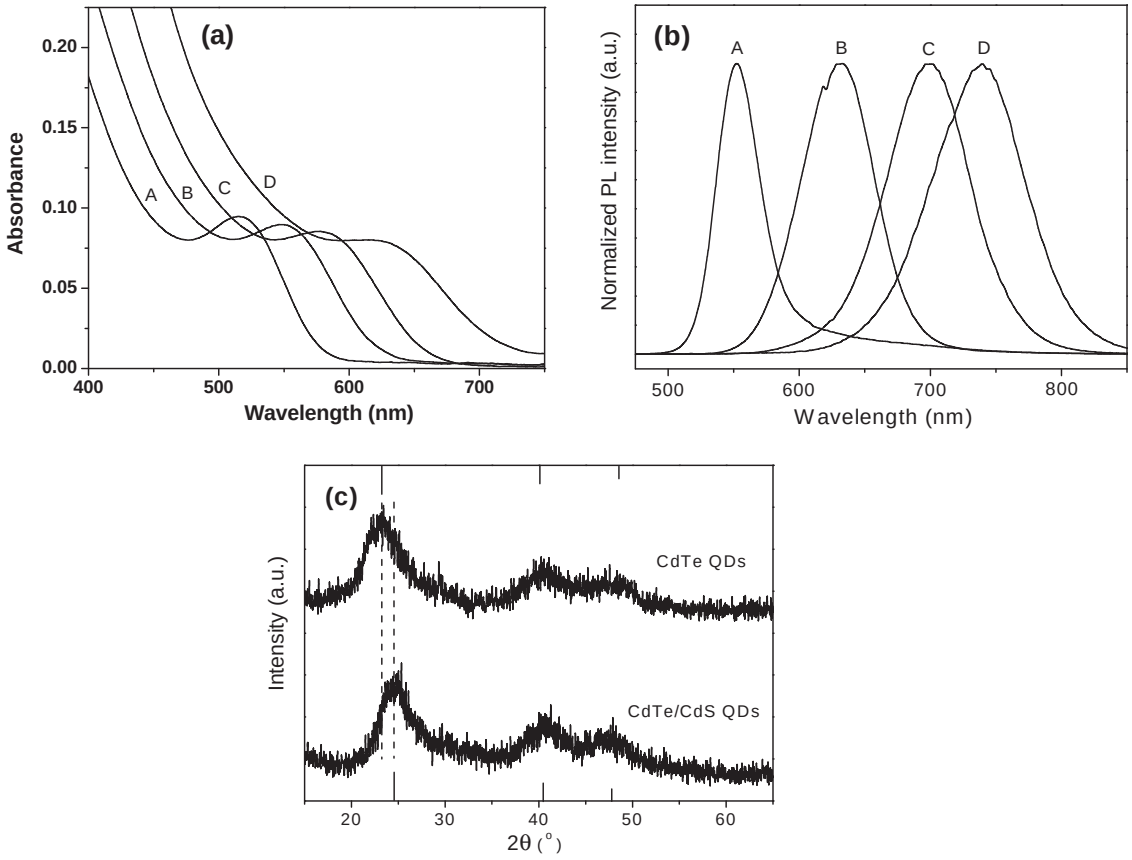

Fig. 1. (a) UV–vis absorption and (b) fluorescence emission spectra of sole core CdTe QDs (A) and CdTe/CdS core/shell QDs with different growth time of CdS layers for 1 h (B), 2 h (C) and 4 h (D), respectively. (c) Powder XRD patterns of sole core CdTe QDs (A) and CdTe/CdS core/shell QDs (D), as referred samples above.

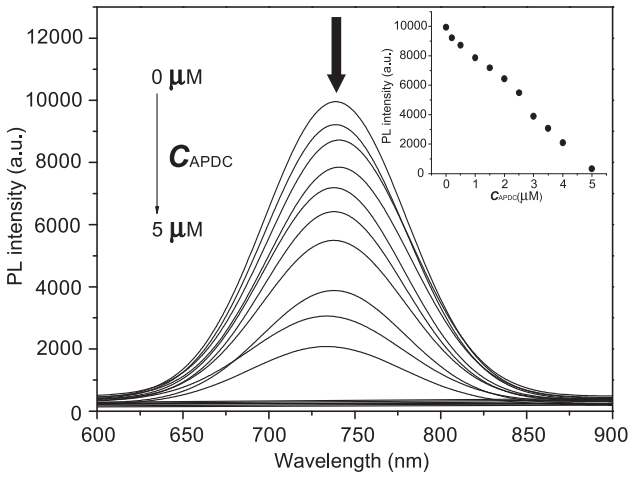

Fig. 2. Fluorescence spectra of CdTe/CdS QDs (sample D) in 10 mM of PBS (pH 7.0) gradually weaken with the each increment of APDC concentration (C_{APDC}) from 0 to 5 μM. The concentration of QDs (C_{QDs}) and excitation wavelength (λ_{ex}) are 20 nM and 600 nm, respectively.

would exhibit a marked narrowing of the XRD peak width upon increasing particles [36]. Hence, this result adequately confirms the formation of core/shell structures rather than an alloyed structure in these NIR-emitting CdTe/CdS QDs.

3.2. APDC-induced PL quenching of CdTe/CdS QDs

As a thiol-capping reagent, MPA is significant for the synthesis of QDs, and efficiently improve water-solubility and stability via forming a Cd–thiol complex around the surface of QDs. This complex layer occupies surface sites and passivates the surface to maintain high-quality PL [37]. Notwithstanding, APDC, utilized as chelating reagents in analytical chemistry [38], partly breaks the complex layer and separates out Cd^{2+}, which is combined by APDC to compose of a new complex (Cd–APDC). That is, partial loss of Cd–thiol complex induces obvious PL quenching. As demonstrated in Fig. 2, the addition of APDC caused remarkable PL quenching of QDs. With the addition of 5 μM of APDC, corresponding PL spectra reduced to be a horizontal line, indicating the appearance of a nearly full PL quenching behavior. Meanwhile, a slight PL spectrum blue-shift (by 8 nm) was observed after adding 4 μM of APDC. This result indirectly testified the occurrence of a reduced diameter due to lacking Cd–thiol complex around surface of QDs, in accordance with size-tuning PL spectra of QDs.

3.3. Cd^{2+}-induced PL enhancement of QDs-APDC

According to primary analysis above, APDC induced PL quenching of CdTe/CdS QDs was attributed to partial loss of the Cd–thiol complex, as surface passivation layers. Consequently, it makes sense for restoring PL of these APDC-modified CdTe/CdS QDs (QDs-APDC) to introduce Cd^{2+} to repair the destroyed surface of QDs by forming Cd–thiol complex again. As illustrated in Fig. 3a, gradually enhanced PL spectra of QDs-APDC were observed in the $C_{Cd^{2+}}$ range from 0 to 2 μM. That is, PL intensity of QDs increased rapidly upon addition of Cd^{2+} in this area. To evaluate PL enhancement efficiency, PL intensity of QDs-APDC after (F) and before (F_0) adding diverse $C_{Cd^{2+}}$ were investigated. As displayed in Fig. 3b, the relationship between PL intensity ratio (F/F_0) and $C_{Cd^{2+}}$ was almost proportional. Corresponding regression equation presented a good linear correlation coefficient (R) of 0.9989 and a low average relative standard deviation of 2.3% (six repeats).

The limit of detection (LOD) of this proposed method was 6 nM, calculated by the 3σ, where σ is the standard deviation for six replicating detections of blank solutions. Furthermore, in this range from 0.1 to 2 μM, a normal concentration level in most detection situations, especially in biological organism [10], the LOD of 6 nM was lower than that of previous organic dyes- and QDs-based PL sensor for measuring Cd^{2+} [4,5,25]. Wu *et al.* designed the EDTA-etched QDs for detecting Cd^{2+}, and this method gave a detection limit of 10 nM [39]. Xu et al. developed a QDs-based "turn-on" fluorescent probe for detection of Cd^{2+} in aqueous media, and the LOD was calculated to be 0.5 μM [40]. These results richly testified that this proposed method, using a NIR-emitting (QDs-APDC)-based PL sensor, was highly sensitive for the detection of $C_{Cd^{2+}}$ in this range, and would be of practical applications in biological systems.

3.4. Selectivity of this (QDs-APDC)-based PL sensor

To investigate the selectivity of this (QDs-APDC)-based PL sensor of Cd^{2+}, a series of interferential experiments were carried out to evaluate Cd^{2+} selective PL responses in the presence of various cations, as competitors. As can be seen in Fig. 4, in gray pillars, PL responses of original QDs to different cations (including Hg^{2+}, Ag^{+}, Cu^{2+}, and so forth) were observed, together with a series of PL quenching. The phenomenon that PL of water-soluble QDs markedly quenched by particular metal ions has been successfully confirmed [29]. Furthermore, PL enhancement behavior could only

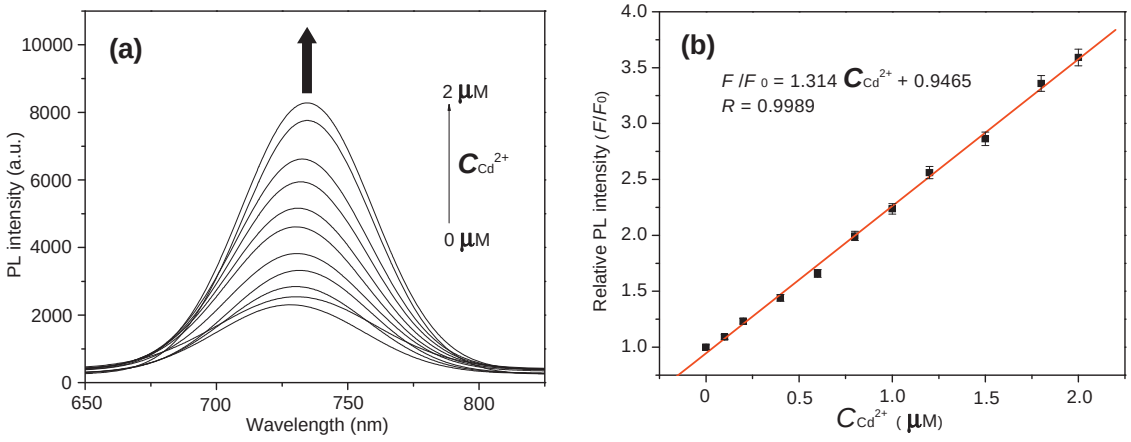

Fig. 3. (a) Fluorescence spectra of CdTe/CdS QDs with addition of 4 μM of APDC recover due to introducing Cd^{2+} in the concentration ($C_{Cd^{2+}}$) range from 0 to 2 μM. (b) Linear relationship of the ratio of PL intensity of QDs-APDC after (F) to that before (F_0) adding various $C_{Cd^{2+}}$ (F/F_0) and $C_{Cd^{2+}}$. Herein, C_{QDs} is 20 nM and λ_{ex} is 600 nm.

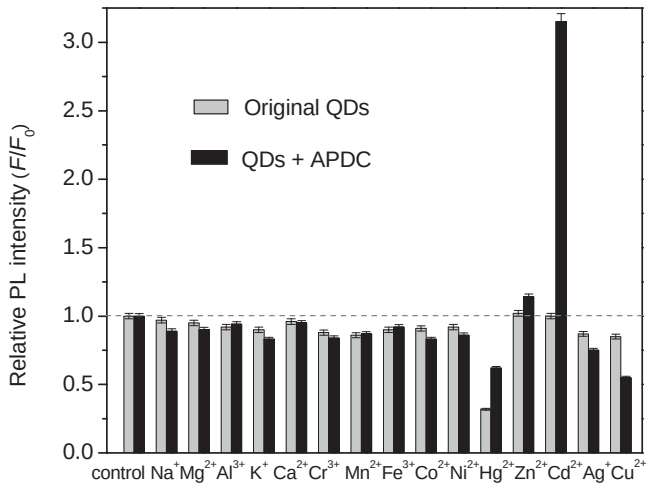

Fig. 4. The ratio of PL intensity of original CdTe/CdS QDs before (F_0) and after (F) adding diverse cations (2 μM) displayed in grey pillars, and that for the case of QDs-APDC showed in black pillars. Therein, C_{QDs}, C_{APDC} and λ_{ex} are 20 nM, 4 μM and 600 nm, respectively.

be achieved in this system after the surface of QDs was modified by APDC.

In black pillars, PL responses of QDs-APDC to diverse cations (except Cd^{2+}) were slight, together with faint PL quenching and enhancement. In detail, only Cd^{2+} resulted in apparent PL enhancement of QDs-APDC, and over 3.2-fold PL increment was observed for the case of Cd^{2+}. In addition, Zn^{2+} could also lead to slightly enhanced PL of QDs-APDC, which was attributed to similar mechanism that the formation of surface passivation layers Zn-thiol (or Cd–thiol) around QDs led to PL enhancement [39]. Nevertheless, the PL enhancement efficiency from Cd^{2+} was much more distinct than that from Zn^{2+} under the same situation. Thus, particular PL responses of the QDs-APDC could be utilized to develop a PL sensor for highly selective detection of Cd^{2+}.

3.5. Mechanism of this (QDs-APDC)-based PL sensor for Cd^{2+}

The introduction of Cd^{2+} apparently enhanced PL of QDs-APDC, which probably result from the formation of Cd–thiol passivation layers on the surface of QDs. To further prove this hypothesis, UV–vis absorption spectra, PL spectra and PL lifetimes of CdTe/CdS QDs and QDs-APDC in the absence and presence of Cd^{2+} were measured. As illustrated in Fig. 5a, characteristic absorption peak of CdTe/CdS QDs was blue shifted to a shorter wavelength owing to the addition of APDC. Similar spetra blue shifts were found in corresponding PL spectra of QDs-APDC (in Fig. 2). These results indicated that APDC-induced PL quenching was due to lacking Cd–thiol complex around QDs, in company with a reduced hydrodynamic diameter, measured by dynamic light scattering (DLS, Supporting information Fig. S1). Dissociative by-products (Cd–APDC), as referred in Scheme 1, were detected by means of the ICP-AES (Table S1). That suggested the occurrence of ligand exchange between MPA and APDC with Cd^{2+} ions around the surface of QDs.

In addition, slight red-shift behavior of QDs-APDC was observed in their absorption and PL spectra upon the addition of Cd^{2+}. In detail, characteristic PL and absorption peak were shifted to a longer wavelength by 6 and 8 nm, respectively, as depicted in Fig. 3a and Fig. 5a. PL intensities of QDs and QDs-APDC bi-exponentially decayed, and average PL lifetime of QDs reduced from 49.9 to 33.1 ns due to adding 4 μM of APDC. This decrease resulted from surface chemical etching of APDC around QDs [39]. By contrast, the average PL lifetime of this QDs-APDC increased from 33.1 to 40.2 ns after introducing 2 μM of Cd^{2+}, as showed in Fig. 5b (detailed data in Table S2). The increased PL lifetime and spectra red-shift of QDs-APDC testified the formation of Cd–thiol complex layers around the surface of these QDs to passivate their surface. According to previous literatures, the surface passivation of nanocrystals (e.g. QDs) with high bandgap materials (e.g. CdS from Cd–thiol) has been confirmed to be a perfect route to improve PL efficiency and stability of nanocrystals [35,41,42].

3.6. Analytical performance of this (QDs-APDC)-based PL sensor

To evaluate analytical performance of this proposed method using a (QDs-APDC)-based PL sensor, a series of detection experiments were implemented in tap water, river water and liposome solutions (as biological samples), respectively. All samples were prepared by intentionally introducing Cd^{2+} at diverse concentration levels, and were determined by this sensor and the standard ICP-AES independently. As summarized in Table 1, all results obtained by the sensor were in good agreement with those measured by the ICP-AES. The relative standard deviation (RSD) of each sample measurement from this sensor was no more than 5%. In general, many common metal cations, as referred in Fig. 4, such as Ca^{2+}, Mg^{2+}, Mn^{2+} and Cu^{2+}, could be present in tap water and river water. Determined results of water samples by the sensor richly

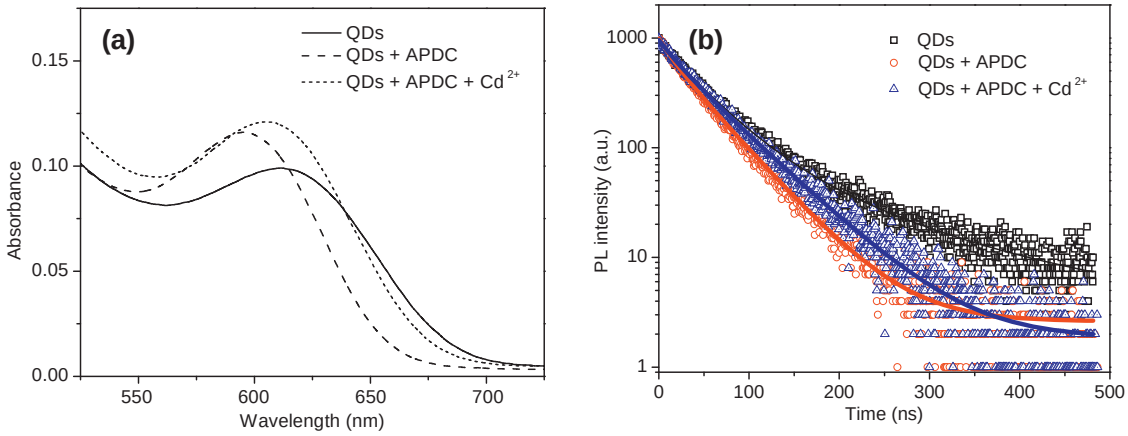

Fig. 5. (a) UV–vis absorption spectra and (b) PL decay curves of CdTe/CdS QDs and QDs-APDC before and after introducing Cd^{2+} ions, as indicated in the legend. The emission was monitored at the first exitonic peak wavelength of corresponding QDs. The PL lifetimes were obtained by bi-exponential curve fitting, inserted as (original QDs) black lines, (QDs-APDC) red lines and (QDs-APDC-Cd^{2+}) blue lines. In all experiments, the C_{QDs}, C_{APDC} and $C_{Cd^{2+}}$ are 20 nM, 4 μM and 2 μM, respectively. (For interpretation of the references to color in figure legend, the reader is referred to the web version of the article.)

Table 1
Analytical results of Cd^{2+} in water samples and liposome solutions from PL sensor and the ICP-AES.

Samples[a]	Added Cd^{2+} (μM)	By PL sensor (μM)	RSD (%)[b]	By ICP-AES (μM)	RSD (%)
Tap water 1	0.050	0.054 ± 0.002	3.704	0.055 ± 0.003	5.454
Tap water 2	0.100	0.095 ± 0.004	4.210	0.105 ± 0.002	1.905
Tap water 3	0.200	0.211 ± 0.009	4.265	0.207 ± 0.005	2.415
River water 1	0.100	0.109 ± 0.005	4.487	0.112 ± 0.006	5.357
River water 2	0.500	0.523 ± 0.017	3.250	0.518 ± 0.011	2.123
River water 3	1.000	1.029 ± 0.025	2.429	1.033 ± 0.015	1.452
Liposome 1	0.100	0.093 ± 0.003	3.226	0.095 ± 0.004	4.210
Liposome 2	0.500	0.489 ± 0.008	1.634	0.507 ± 0.013	2.564
Liposome 3	1.000	1.055 ± 0.034	3.223	0.985 ± 0.026	2.640

[a] All concentrations were expressed as mean of five determinations ± standard deviation (SD).
[b] The relative standard deviation (RSD) was calculated as (SD/mean) × 100%.

testified that these cations hardly interfere with the detection of Cd^{2+}. In addition, the sensor also displayed a great tolerance in complicated systems. Almost accordant results from the determination of liposome solutions, using the two technologies independently, effectively proved the practicability of the sensor in biological samples. Consequently, the coexistence of other interferential metal ions and biological molecules in practical sample systems hardly affect the detection of Cd^{2+}.

4. Conclusions

A facile NIR-emitting CdTe/CdS core/shell QDs-based PL sensor was developed to detect Cd^{2+} in aqueous media. This sensor was based on a PL "OFF–ON" mode. With the introduction of APDC, initial PL of QDs was markedly quenched, which was ascribed to APDC induced partial breakage of surface Cd–thiol layers and the formation of Cd–APDC complex around QDs. Upon addition of Cd^{2+}, PL enhancement behavior of QDs-APDC was observed, which was attributed to the occurrence of Cd–thiol passivation layers again on the surface of QDs, together with restoring of the PL. Experimental results testified that PL of QDs-APDC was almost proportional toward $C_{Cd^{2+}}$ in the range from 0.1 to 2 μM. Corresponding regression equation showed a good correlation coefficient of 0.9989 and a low RSD of 2.3% ($n = 6$). The LOD of this proposed method (6 nM) was lower than that of other QDs and organic dyes-based PL sensor of Cd^{2+} in the same situation. In addition, the sensor of Cd^{2+} was highly selective over other metal ions. Determined results of water samples and liposome solutions by this sensor were in good agreement with those by the ICP-AES. It meant that the coexistence of other metal ions and biological molecules hardly affect the detection of Cd^{2+}. Thus, this proposed sensor of Cd^{2+} was highly sensitive and selective, and would be promising for practical applications in diverse water samples and biological systems.

Acknowledgments

This work was financially supported by the National Natural Science Foundation of China (Nos. 20673059 and 20573056), the Nature Science Keystone Foundation of Shanghai (08jc1408100), the Nanotechnology Special Program Foundation of Shanghai (0652nm010), and the Fundamental Research Funds for the Central Universities of China (WK0913002).

Appendix A. Supplementary data

Supplementary data associated with this article can be found, in the online version, at http://dx.doi.org/10.1016/j.talanta.2012.03.036.

References

[1] S. Dobson, Cadmium: Environmental Aspects, World Health Organization, Geneva, 1992.
[2] M.J.S. McLaughlin, B.R. Singh, Cadmium in Soils and Plants, Kluwer, Dordrecht, 1999.
[3] G.F. Nordberg, R.F.M. Herber, L. Alessio, Cadmium in the Human Environment, Oxford University Press, Oxford, UK, 1992.
[4] T. Cheng, Y. Xu, S. Zhang, W. Zhu, X. Qian, L. Duan, J. Am. Chem. Soc. 130 (2008) 16160–16161.
[5] Y. Bao, B. Liu, H. Wang, F. Du, R. Bai, Anal. Methods 3 (2011) 1274–1276.
[6] Y. Oztekin, A. Ramanaviciene, N. Ryskevic, Z. Yazicigil, Z. Ustundag, A.O. Solak, A. Ramanavicius, Sens. Actuators B 157 (2011) 146–153.
[7] A.R. Clapp, I.L. Medintz, J.M. Mauro, B.R. Fisher, M.G. Bawendi, H. Mattoussi, J. Am. Chem. Soc. 126 (2004) 301–310.
[8] C.Y. Zhang, H.C. Yeh, M.T. Kuroki, T.H. Wang, Nat. Mater. 4 (2005) 826–831.
[9] M.G. Sandros, D. Gao, D.E. Benson, J. Am. Chem. Soc. 127 (2005) 12198–12199.
[10] J. Liu, C. Bao, X. Zhong, C. Zhao, L. Zhu, Chem. Commun. 46 (2010) 2971–2973.
[11] V.V. Matylitsky, L. Dworak, V.V. Breus, T. Basché, J. Wachtveitl, J. Am. Chem. Soc. 131 (2009) 2424–2425.
[12] M. Xue, X. Wang, H. Wang, D. Chen, B. Tang, Chem. Commun. 47 (2011) 4986–4988.
[13] S. Huang, Q. Xiao, Z.K. He, Y. Liu, P. Tinnefeld, X.R. Su, X.N. Peng, Chem. Commun. (2008) 5990–5992.
[14] Q. Zhao, F. Li, C. Huang, Chem. Soc. Rev. 39 (2010) 3007–3030.
[15] G. Liang, H. Liu, J. Zhang, J. Zhu, Talanta 80 (2010) 2172–2176.
[16] N. Butwong, T. Noipa, R. Burakham, S. Srijaranai, W. Ngeontae, Talanta 85 (2011) 1063–1069.
[17] E.M. Ali, Y.G. Zheng, H.H. Yu, J.Y. Ying, Anal. Chem. 79 (2007) 9452–9458.
[18] Y.S. Xia, C.Q. Zhu, Analyst 133 (2008) 928–932.
[19] H.B. Li, Y. Zhang, X.Q. Wang, D.J. Xiong, Y.Q. Bai, Mater. Lett. 61 (2007) 1474–1477.
[20] S.G. Ge, C.C. Zhang, Y.N. Zhu, J.H. Yu, S.S. Zhang, Analyst 135 (2010) 111–115.
[21] E.M. Nolan, S.J. Lippard, Chem. Rev. 108 (2008) 3443–3480.
[22] L. Shang, L. Zhang, S. Dong, Analyst 134 (2009) 107–113.
[23] B. Han, J. Yuan, E. Wang, Anal. Chem. 81 (2009) 5569–5573.
[24] J.L. Chen, C.Q. Zhu, Anal. Chim. Acta 546 (2005) 147–153.
[25] S. Banerjee, S. Kar, S. Santra, Chem. Commun. (2008) 3037–3039.
[26] M.J. Ruedas-Rama, E.A.H. Hall, Anal. Chem. 80 (2008) 8260–8268.
[27] J.M. Costa-Fernandez, Anal. Bioanal. Chem. 384 (2006) 37–40.
[28] J.M. Klostranec, W.C.W. Chan, Adv. Mater. 18 (2006) 1953–1964.
[29] G.X. Liang, H.Y. Liu, J.R. Zhang, J.J. Zhu, Talanta 80 (2010) 2172–2176.
[30] Z. Gu, L. Zou, Z. Fang, W. Zhu, X. Zhong, Nanotechnology 19 (2008) 135604–135610.
[31] L. Zou, Z. Gu, N. Zhang, Y. Zhang, Z. Fang, W. Zhu, X. Zhong, J. Mater. Chem. 18 (2008) 2807–2815.
[32] Z. Fang, L. Liu, J. Wang, X. Zhong, J. Phys. Chem. C 113 (2009) 4301–4306.
[33] W.W. Yu, L. Qu, W. Guo, X. Peng, Chem. Mater. 15 (2003) 2854–2860.
[34] A.M. Smith, A.M. Mohs, S. Nie, Nat. Nanotechnol. 4 (2009) 56–63.
[35] W. Zhang, G. Chen, J. Wang, B.C. Ye, X. Zhong, Inorg. Chem. 48 (2009) 9723–9731.
[36] D.V. Talapin, I. Mekis, S. Gotzinger, A. Kornowshi, O. Benson, H. Weller, J. Phys. Chem. B 108 (2004) 18826–18831.
[37] C.L. Wang, H. Zhang, J.H. Zhang, N. Lv, M.J. Li, H.Z. Sun, B. Yang, J. Phys. Chem. C 112 (2008) 6330–6336.
[38] X.P. Yan, Y. Jiang, Trends Anal. Chem. 20 (2001) 552–562.
[39] P. Wu, X.P. Yan, Chem. Commun. 46 (2010) 7046–7048.
[40] H. Xu, R. Miao, Z. Fang, X. Zhong, Anal. Chim. Acta 687 (2011) 82–88.
[41] B.O. Dabbousi, J. Rodriguez-Viejo, F.V. Mikulec, J.R. Heine, H. Mattoussi, R. Ober, K.F. Jensen, M.G. Bawendi, J. Phys. Chem. B 101 (1997) 9463–9475.
[42] R. Xie, U. Kolb, J. Li, T. Basché, A. Mews, J. Am. Chem. Soc. 127 (2005) 7480–7488.